

Searches at LHC Beyond the Standard Model

Sebastiano Albergo on behalf of the ATLAS and CMS Collaborations*
University of Catania and INFN Catania, Italy

The discovery potentials of ATLAS and CMS experiments at the Large Hadron Collider (LHC) for Supersymmetry (SUSY), Extra Dimensions (ED), new Gauge Bosons and R-Hadrons are discussed. Beyond Standard-Model (BSM) searches at LHC require a detailed understanding of the detector performance, reconstruction algorithms and triggering. Precision measurements of Standard Model (SM) processes are also mandatory to acquire the necessary knowledge of SM background. Both ATLAS and CMS efforts are hence addressed to determine the best calibration candles and to design a realistic plan for the initial period of data taking.

I. INTRODUCTION

ATLAS [1] and CMS [2] are the two general purpose detectors which are being installed at LHC for new physics studies in the TeV Mass range. One of the main goals of ATLAS and CMS is to search for Beyond Standard Model (BSM) signals. The Standard Model [3] provides a successful description of the existing data but it is considered as a low-energy effective theory with some intrinsic deficiencies. The most appealing extension of the SM is SUSY [4]. It proposes an elegant solution to the "hierarchy" problem [4] and provides a good candidate for the dark matter in cosmology, though at the expense of additional parameters of the theory.

Much interest has been produced by other BSM models which hypothesize more than four space-time dimensions. Some of these Extra Dimension models [5, 6, 7, 8] lead to a gravity mass scale in the TeV range, hence predicting relevant signatures in collider particle physics.

Only some of the BSM signatures which will be addressed at LHC are discussed here. Section 2 is devoted to some relevant topics in detector alignment and calibration; Section 3 is devoted to SUSY searches; Section 4 reports some Extra-Dimension discovery potentials and the Z' sensitivity of ATLAS and CMS in the dimuon decay channel.

II. DETECTOR ALIGNMENT AND CALIBRATION

The development of alignment, calibration and commissioning procedures is of primary importance to achieve a good understanding of the detector. For this reason, both the Collaborations are strongly involved in the study of suitable start-up strategies. In this Section, the CMS alignment method is discussed. Results from calibration studies ($t\bar{t}$ "candle") performed by ATLAS are also discussed. Both items well represent the many efforts performed by ATLAS and CMS to face the challenging initial phase of data taking.

A. CMS alignment

The alignment uncertainties of the CMS Tracker and Muon detectors affect the performances of the track pattern recognition and reconstruction. Since the detector alignment is expected to progressively improve with integrated luminosity, different scenarios are usually considered. Here are summarized the two scenarios concerned with data taking:

- First Data Scenario : corresponding to the very early stage of data taking, it should be reached before accumulating $100pb^{-1}$. It assumes 1 mm and 0.2 mrad of relative positioning precision between the Tracker and

* Presented at the HEP MAD-07 Conference

Muon System. Muon Chambers are located within the Muon System to 1 mm and 0.25 mrad precision. The Tracker structure and modules relative misalignment ranges from 3 to 13 μm for the Pixel Detector and from 50 to 300 μm for the Silicon Strip Detector (SSD).

- Long Term Scenario : corresponding to the situation of optimal alignment performance, it is expected after collecting about 1fb^{-1} . In this scenario the Tracker to Muon System relative misalignment will be of 200 μm and 50 mrad, while the SSD precision is improved by a factor 10 with respect to the previous scenario.

The integrated luminosity estimated for each alignment scenario are related to the number of tracks originated from $Z \rightarrow \mu\mu$ and $W \rightarrow \mu\nu$ decays, which are used for track based alignment.

Fig. 1 and Fig. 2 reports the invariant mass distribution of $Z \rightarrow \mu\mu$ events for First Data scenario and Long Term scenario respectively. The study [9] is done using simulated events produced by OSCAR [10], a Monte Carlo program based on GEANT4 which fully simulates the passage of particles through the detector taking into account a detailed description of detector geometry, materials and magnetic field. Digitization of signal generated by simulated particles is done within the framework of the ORCA [11] package, which is also used for the event reconstruction.

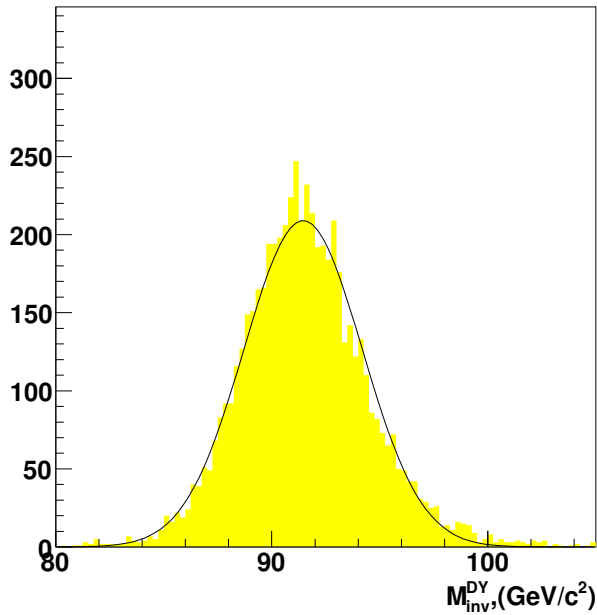


FIG. 1: $Z \rightarrow \mu\mu$ mass peak at “First Data Scenario”. $\sigma_M/M = 0.0226$.

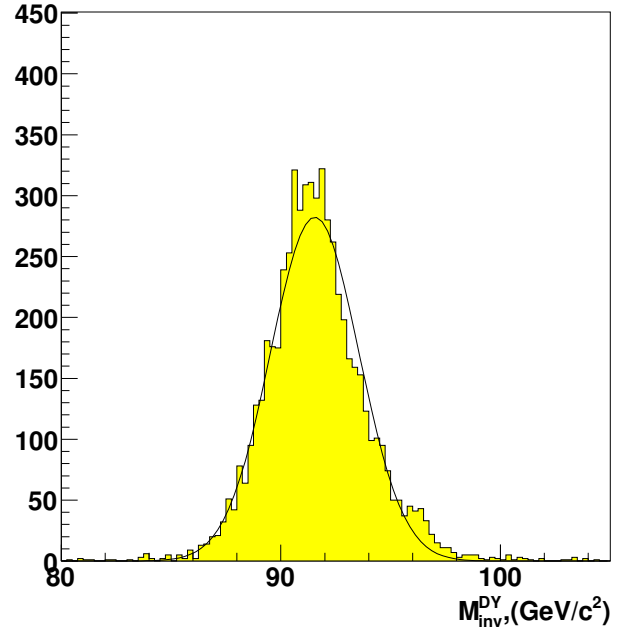


FIG. 2: $Z \rightarrow \mu\mu$ mass peak at “Long Term Scenario”. In this case $\sigma_M/M = 0.0118$, which is comparable to the value 0.0106 obtained in the “ideal alignment” (i.e. no misalignment) case [9].

B. $t\bar{t}$ calibration candle

The top pair production process is very valuable for the in-situ calibration of the ATLAS and CMS detectors during the first period of data taking. The top quark decays for nearly 100% to W+b. The lepton-plus-jet channel, $t\bar{t} \rightarrow WWb\bar{b} \rightarrow (l\nu)(jj)(b\bar{b})$ has a branching ratio of 29.6%. The large cross section and the large signal to background (S/B) ratio for the lepton+jets $t\bar{t}$ -decay channel, allow to select high purity samples with good statistics with small integrated luminosity. These first collected top data samples will be used to understand some important performance issues like: detector uniformity, absolute energy scale calibration, missing transverse energy calibration, b-tagging, etc. In addition, with these top samples the Monte Carlo can be tuned and the background understanding can be improved.

In the worst initial scenario of absence of b-tagging the largest irreducible contribution to the background originates from W+4 jet events, where the W-boson decays leptonically and produces an isolated lepton and missing transverse energy (\cancel{E}_T), and the four jets survive the selection criteria. In this scenario the $t\bar{t}$ candidate events can be selected [12] requiring:

- one isolated lepton (electron or muon) with $P_T > 20$ GeV/c
- $\cancel{E}_T > 20$ GeV
- 4 reconstructed-jets with constrained cone sizes, each with $-2.5 < \eta < 2.5$ and $P_T > 40$ GeV/c.

In Fig. 3 the resulting top mass peak for 150 pb^{-1} of integrated luminosity in ATLAS is shown [12]. An effective method for absolute energy scale calibration relies on the W mass peak reconstruction, by taking advantage of the well known experimental value of the W mass. The W candidates can be selected from the top event set by requiring the two jets with highest P_T . Plotting the two-jet invariant mass distribution a clear W peak is resolved (see Fig. 4).

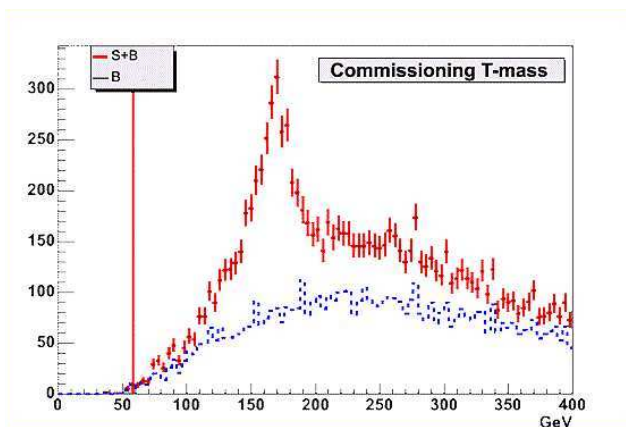


FIG. 3: Top reconstructed mass with 150 pb^{-1} of integrated luminosity in ATLAS.

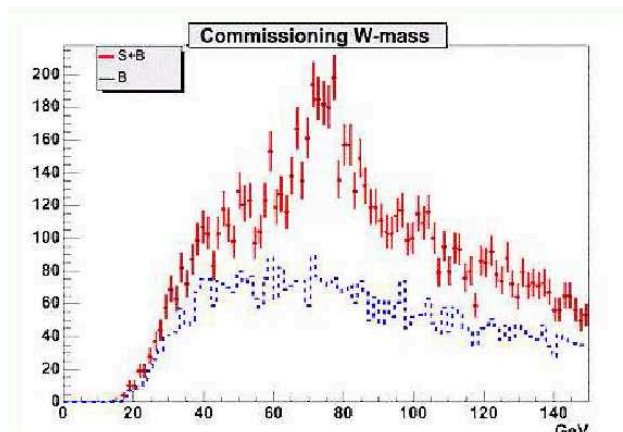


FIG. 4: W reconstructed mass with 150 pb^{-1} of integrated luminosity in ATLAS.

III. SUPERSIMMETRY

The LHC potentials to discover SUSY are mainly analysed in the more constrained framework of the Minimal Supergravity (mSUGRA) [13] model with only 5 free parameters: the common scalar (m_0) and fermion ($m_{1/2}$) masses, the trilinear coupling (A_0) and the Higgs sector parameters ($\tan\beta$, $\text{sgn}\mu$) at the Grand Unification (GUT) scale. Assuming R-parity, new supersymmetric particles are produced in pairs and the lightest one, namely the Lightest Supersymmetric Particle (LSP), is stable and neutral.

A. Inclusive signatures

At the LHC, the SUSY production is dominated by strongly interacting squarks and gluinos, which have long decay cascades with the jet emission. The cascade ends with the LSP, which is not detected. Therefore, the most generic SUSY signature is a multi-jet with large \cancel{E}_T final state. Leptons produced in decays of charginos or neutralinos can also be present, hence also final states with ($n \geq 1$ leptons)+jets+ \cancel{E}_T are considered. The main backgrounds are QCD and $t\bar{t}$, W and Z with QCD-jet associated production processes. Finally, diboson production, such as WW+jets, WZ+jets, and ZZ+jets, also contribute as sources of background. Considering signatures with at least one lepton, substantially reduces the QCD background.

Due to the very high QCD production cross section, the main background for the jets+ \cancel{E}_T channel is dominated by QCD events with large missing transverse energy resulting from jet mismeasurements and detector resolution effects. Topological variables are used to reduce as much as possible the QCD background, in particular the angular correlation between the first two jets (ordered in E_T) and the \cancel{E}_T direction is used.

The inclusive SUSY searches employ the following strategy [14]. First, experimental signatures are studied for a limited number of test points of mSUGRA parameter space using the full simulation and reconstruction software.

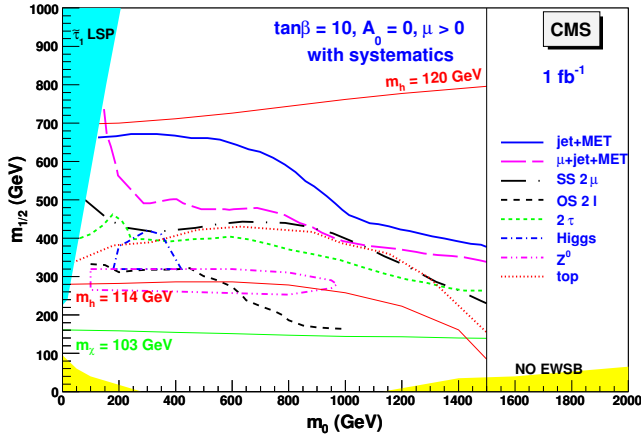


FIG. 5: The mSUGRA discovery reach in the $(m_0-m_{1/2})$ plane for fixed $A_0 = 0$, $\tan\beta = 10$, $\mu > 0$ for 1 fb^{-1} of collected data for several search strategies studied by CMS (including systematic uncertainties) as presented in Ref. [14].

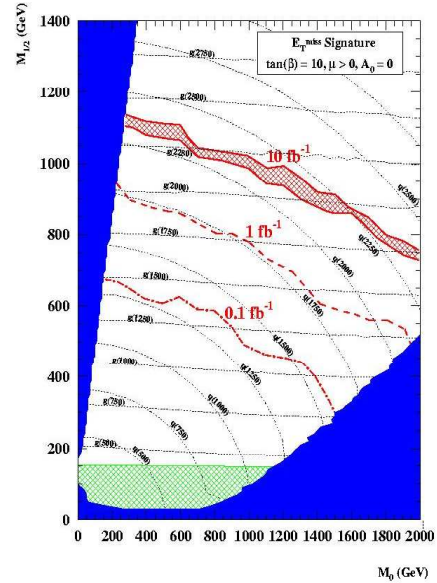


FIG. 6: The mSUGRA discovery reach of ATLAS for the jets+ \cancel{E}_T inclusive channel in the $(m_0-m_{1/2})$ plane for fixed $A_0 = 0$, $\tan\beta = 10$, $\mu > 0$ and for different values of integrated luminosity.

Next, the results are extended to other points of the parameter space. using fast simulation and reconstruction. In order to obtain the best signal to background (S/B) ratio the SUSY selection cuts are optimised for each point. The expected discovery reach is evaluated for parameter sets having at least five standard deviation (5σ) signal significance. As shown in Fig. 5, referred to CMS, several different final states have been considered [14].

As can be seen in Fig. 6, where the ATLAS discovery potential for the jets+ \cancel{E}_T inclusive channel is shown, a huge region of the parameter space can be exploited already with low integrated luminosity.

The multi-jets + \cancel{E}_T final state is expected to be the most sensitive SUSY-search strategy.

Signatures involving at least one lepton are less sensitive, but experimentally cleaner and have the advantage of an efficient and well-understood trigger shortly after LHC start-up. Topological requirements on the jets and missing energy are similar to the fully inclusive analysis.

B. Semi-inclusive and esclusive searches

Exclusive SUSY searches consist in reconstruction of specific decay channels in order to estimate physical parameters characterising the decay itself. Due to the presence of the invisible LSP, a direct determination of the sparticle masses involved in the decay is not possible at LHC. A well established technique to achieve this goal exploits the presence of kinematic properties (end points and thresholds) in the invariant mass distribution of various subsets of particles (usually leptons and quarks and their combinations) [15]. This kind of analysis is able to give strong constraints on mass spectrum and SUSY parameters.

Using similar cuts of the inclusive case and looking for same flavour opposite sign (SFOS) dilepton pairs provides a clean SUSY signature. The SFOS dilepton final state is particularly interesting since leptons (electrons and muons) from the $\tilde{\chi}_2^0$ decay exhibit a peculiar l^+l^- invariant mass distribution with a sharp edge, as shown for CMS in Fig. 7 at the parameter point LM1 ($m_0 = 60 \text{ GeV}/c^2$, $m_{1/2} = 250 \text{ GeV}/c^2$, $\tan\beta = 10$, $A_0 = 0$, $\mu > 0$) in a full simulation and reconstruction study [16]. The reconstruction of the dilepton edge provides information on the sparticles involved in the decay chain and constitute a powerfull indication of new physics especially in the early data taking period.

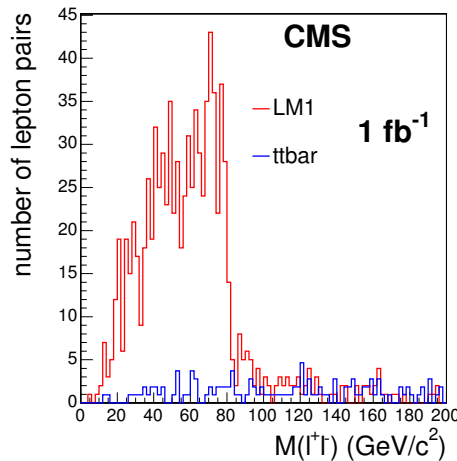


FIG. 7: Same flavour opposite sign lepton pair distributions of SUSY and $t\bar{t}$ events for 1 fb^{-1} . The peculiar triangular edge is clearly visible at point LM1.

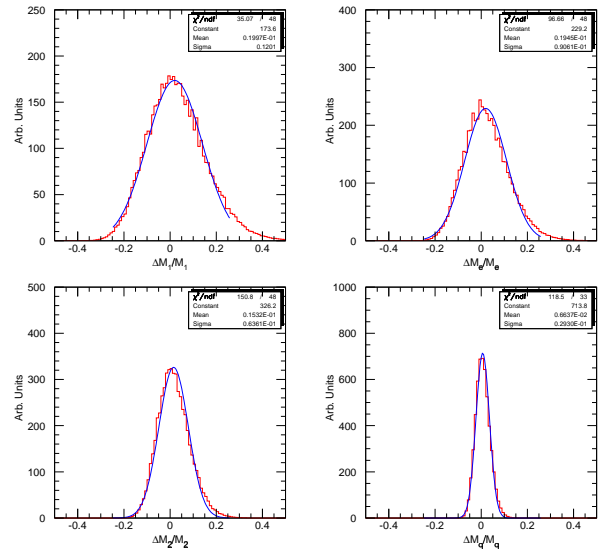


FIG. 8: Distribution of the $\tilde{\chi}_1^0$, \tilde{l}_R , $\tilde{\chi}_2^0$ and \tilde{q}_L invariant masses at 70 fb^{-1} of integrated luminosity. The fitted width are $\pm 12\%$, $\pm 9\%$, $\pm 6\%$ and $\pm 3\%$ respectively.

In Ref. [17] an exclusive study is presented which shows an example of sparticle mass reconstruction with the ATLAS detector in the three-step decay chain $\tilde{q}_L \rightarrow \tilde{\chi}_2^0 q \rightarrow \tilde{l} l q \rightarrow \tilde{\chi}_1^0 l^+ l^- q$. The simulated data corresponds to about 70 fb^{-1} of integrated luminosity and are generated in the mSUGRA framework with parameter values $m_0 = 100 \text{ GeV}/c^2$, $m_{1/2} = 300 \text{ GeV}/c^2$, $A_0 = 300 \text{ GeV}$, $\tan\beta = 2$, $\text{sgn}\mu = +$. Suitable cuts are adopted on \cancel{E}_T , on the number of jets and isolated leptons and on their P_T and η values. The reconstructed edges of ll , lq and llq invariant mass distribution together with the llq threshold are obtained in order to extract, by fitting procedure, the resulting $\tilde{\chi}_1^0$, \tilde{l}_R , $\tilde{\chi}_2^0$ and \tilde{q}_L mass distributions. In order to properly account the uncertainties on the four end-point values, a huge number of randomly generated sets of \tilde{l}_R , $\tilde{\chi}_2^0$ and \tilde{q}_L mass values has been produced. Each set has been weighted depending on the dispersion on the kinematically related $\tilde{\chi}_1^0$ mass values. Resulting mass histograms are shown in Fig. 8.

C. R-Hadrons

Different SUSY models predict long-lived sparticles which can hadronize with normal quarks or gluons forming heavy hadrons, named R-Hadrons. Split Supersymmetry models (Split SUSY [18]) predict a long lived gluino. The existence of a long lived stop is hypotesized in some SUSY-5D [19]. The new long-lived hadrons are expected to have lifetime high enough to cross the detector and a mass higher then $\sim 100 \text{ GeV}/c^2$. R-hadrons can flip their electric charge in hadronic interactions when crossing the detector. Being massive these particles are slow in spite of a high momentum and their specific energy loss is much higher, at a given momentum, than ordinary particles.

It has been shown with a fast simulation study [20] that calorimeter measurements could be used to identify R-hadrons. In Fig. 9 particle distributions vs E/P ratio for different kind of incident particles impinging the ATLAS barrel calorimeters are plotted.

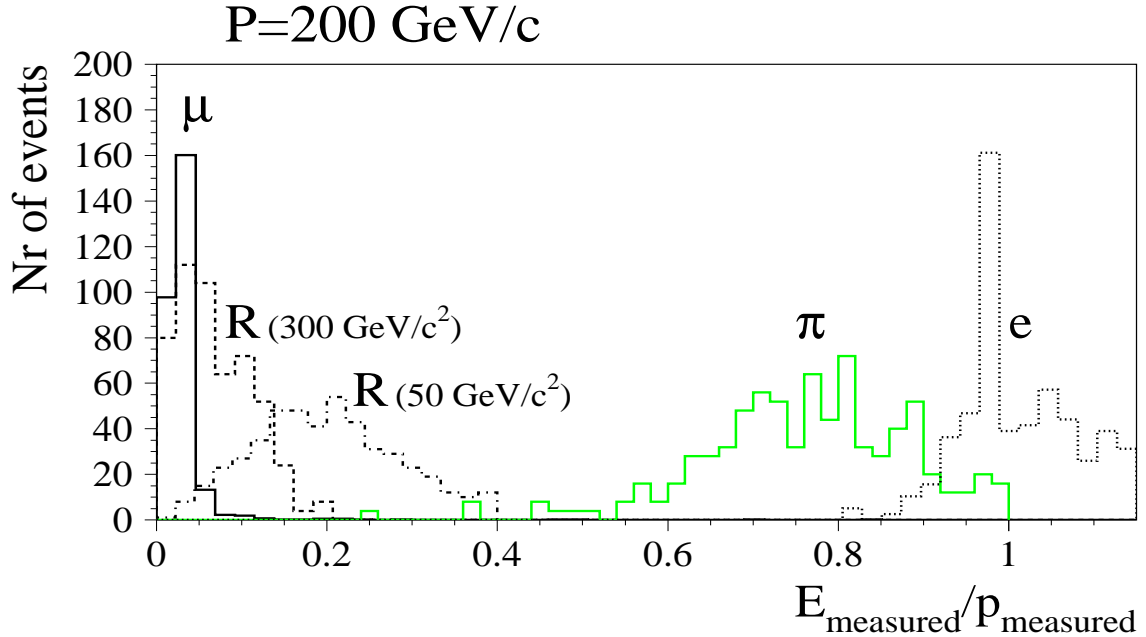


FIG. 9: The ratio E/p for R-hadrons, muons, pions and electrons $\eta = 0.1$. Singly charged R-mesons, muons, pions and electrons are generated and reconstructed in fast simulation.

Another ATLAS study [21] performs the reconstruction of gluino R-hadron masses with a method [22] based on time of flight measurements, while, together with the time of flight method, a complementary approach [23] is studied in CMS. This approach is based on the specific energy loss measurement inside the CMS silicon tracker. R-hadron velocity is then indirectly obtained by inverting the Bethe-Bloch formula in the range $0.1 < \beta < 0.9$.

IV. OTHER BSM SEARCHES

A. Gravitons

The production of Kaluza-Klein gravitons in high energy particle collision is predicted in various extra dimensional scenarios. Presently the most popular extra dimensional models in high energy physics are the Arkani-Hamed, Dimopoulos and Dvali (ADD) [5]; the Randall Sundrum (RS) [6]; the TeV^{-1} Size Extra Dimensions [7]; and the Universal Extra Dimensions (UED) [8].

The ADD model has large compactified extra dimensions, in which gravity can propagate, while the SM particles are confined to the usual 4-dimensional space-time brane. In the RS model, the hierarchy problem is solved by having a single highly curved (warped) extra dimension. In this scenario, gravity is localized on one brane in the extra dimension, while the SM particles are located on another. In the TeV^{-1} Size Extra Dimensional Model, the SM chiral fermions are confined to a brane or branes, but the SM gauge bosons (W, Z, γ and g) can propagate into the extra dimensions. In UED, all SM fields are allowed to propagate along EDs. Therefore, each SM particle has Kaluza-Klein excitations.

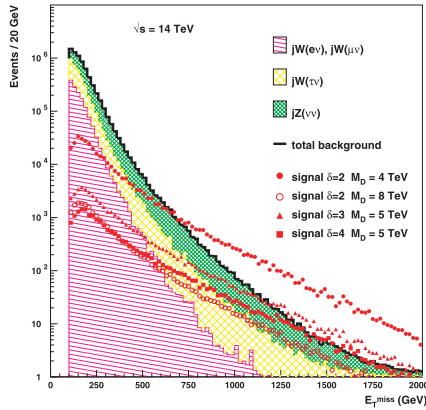


FIG. 10: \cancel{E}_T distribution in ATLAS of background events and of ADD-graviton signal events after data selection, for 100 fb^{-1} of integrated luminosity. The contribution of the three main kinds of background is shown as well as the distribution of the signal for several values of the model parameters.

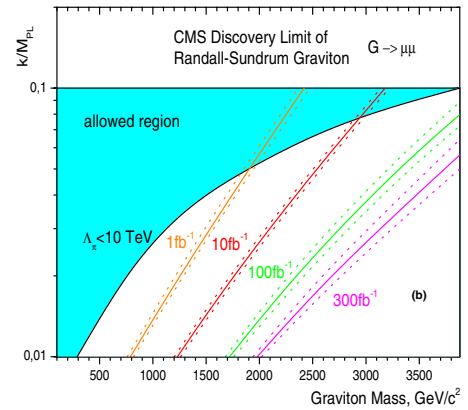


FIG. 11: CMS Discovery limit for RS graviton as a function of the model parameter k and the graviton mass for various values of integrated luminosity. The left part of each curve is the region where significance exceeds 5σ . The ranges of the expected variations due to the systematic uncertainties are shown.

All these models have signatures which are potentially detectable at accelerators. In particular ADD and RS models predict evident signatures based on direct graviton production. An emission of a massless graviton in association with a jet is predicted by ADD, so a clear signature of back-to-back jet+ \cancel{E}_T is expected. In which the \cancel{E}_T is related to gravitons emitted into the extra dimensions, which consequently escape detection. The dominant backgrounds arise from processes that can give rise to neutrinos in the final state, namely $\text{jet}+Z \rightarrow \nu\nu$, $\text{jet}+W \rightarrow \tau\nu$, $\text{jet}+W \rightarrow \mu\nu$ and $\text{jet}+W \rightarrow e\nu$. By vetoing the events where there is an isolated lepton within the acceptance of the ATLAS muon or tracking systems the background from the last two sources is reduced. Fig. 10 shows [24] the \cancel{E}_T distribution of the backgrounds and of the signals in ATLAS for several choices of the number of extra dimensions δ and the model parameter M_D . The signal emerges from the background at large \cancel{E}_T . The distributions for the different signals reflect the expected scaling of the cross section as a function of $M_D^{-\delta-2}$.

The RS model graviton can decay in the dilepton, dijet or diboson channel. In the dilepton case the signature would be a series of narrow resonances in the dilepton invariant mass distribution. The dominant background arises from the Drell-Yan lepton pair production, whereas contributions from $t\bar{t}$ and the vector boson pair production (ZZ ,

WZ, WW) are significantly smaller and are highly suppressed by selection cuts. The CMS discovery limit [14] for this channel is shown in Fig. 11 for 1, 10, 100 and 300 fb⁻¹ of integrated luminosity.

B. New Gauge bosons

Extra Gauge Bosons Z' and W' are predicted by several different models, generally belonging to the following classes [25]:

- Superstring inspired and Grand Unification theories (GUT);
- Left-Right Symmetric Models based on the gauge group $SU(3)_{C} \times SU(2)_{L} \times SU(2)_{R} \times U(1)_{B-L}$ predicting sub-structures of the known elementary particles;
- Little Higgs Models.

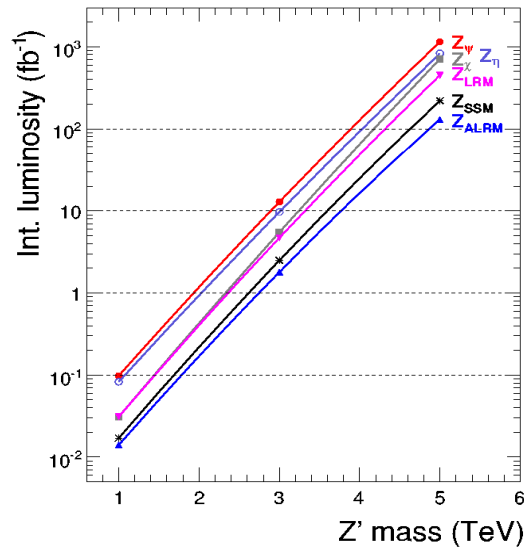


FIG. 12: Integrated luminosity needed to reach 5 σ significance in the $Z' \rightarrow \mu\mu$ channel. lines are the results of interpolations between the points.

The dimuon decay is a golden channel for Z' discovery. As for the RS graviton decay in dilepton, also in the case of Z' the dominant background arises from the Drell-Yan lepton pair production, whereas contributions from $t\bar{t}$ and from the vector boson pair production (ZZ, WZ, WW) are significantly smaller and are highly suppressed by selection cuts. The momentum resolution of the detector plays a key role in separating the signal from the background. New reconstruction algorithms have been developed to increase the lepton reconstruction efficiency. In particular for very high- p_T muons, the track fitting in the tracker and in the muon system are optimised to detect and correct effects of their energy loss. Results of a study [14] obtained with full simulation and reconstruction of signal and background is shown in Fig. 12, where the discovery potential of Z' at CMS in the dimuon channel is shown for six different model predictions.

V. CONCLUSIONS

The initial phase of running will be crucial both for ATLAS and CMS: the detectors have to be understood and calibrated and the SM processes have to be measured. After this huge starting program has been done, exciting

searches for new physics can be performed. The LHC collaborations are getting ready for this fascinating period, by validating the software and preparing data analysis while installing and commissioning the detector. In several discovery channels considered up to now, it has been demonstrated that, also including systematic uncertainties, signals of new physics could already manifest with an integrated luminosity lower than 1 fb^{-1} . The analysis effort in the next few months before the start of LHC will be devoted to further develop robust selection criteria and analysis methods to avoid biases due to the large systematic uncertainties that we will have at the beginning.

References

- [1] ATLAS Collaboration, CERN-LHCC-94-43
- [2] CMS Collaboration, CERN-LHCC-94-38
- [3] S.L. Glashow 1961 *Nucl. Phys.* **22** (1961) 579-588; S. Weinberg *Phys. Rev. Lett.* **19** (1967) 1264-1266
- [4] H.P.Nilles *Phys. Rept.* **110** (1984) 1
- [5] N. Arkani-Hamed, S. Dimopoulos and C. Dvali, *Phys. Lett. B* 429 (1998) 261.
- [6] L. Randall and R. Sundrum, *Phys. Rev. Lett.* 83 (1999) 3370-3373; L. Randall and R. Sundrum, *Phys. Rev. Lett.* 83 (1999) 4690-4693.
- [7] I. Antoniadis, *Phys. Lett.* B246 (1990) 377-384.
- [8] K. Kong, K. T. Matchev, hep-ph/0610057 (2006)
- [9] I. Belotelov et al., CMS NOTE 2006/017
- [10] CMS Collaboration, CMS Simulation Package, <http://cmsdoc.cern.ch/oscar>.
- [11] CMS Collaboration, CMS Reconstruction Package, <http://cmsdoc.cern.ch/orca>.
- [12] S.Bentvelsen and M.Cobal, ATL-PHYS-PUB-2005-024
- [13] L. Alvarez-Gaume , J. Polchinski and M.B.Wise *Nucl. Phys.* **B221** (1983)495
- [14] CMS Physics T.D.R. Vol.2, CERN-LHCC-2006-021
- [15] B C Allanach, C Lester, M A Parker and B Webber, *J. High Energy Phys.* 9 (2000) 4.
- [16] M.Chiorboli , M.Galanti and A.Tricomi, CERN-CMS-NOTE-2006-133
- [17] H.Bachacon, I.Hinchliffe and F.E. Paige, ATL-COM-PHYS-99-017
- [18] G. F. Giudice and A. Romanino, *Nucl. Phys. B* 699 (2004) 65, [Erratum-ibid. B 706 (2005) 65]
- [19] R.Barbieri, G.Marandella and M.Papucci, *Phys.Rev.D* 66 (2002) 095003
- [20] A.C.Kraan, J.B.Hansen, P.Nevski, arXiv:hep-ex/0511014v3
- [21] S. Hellman, M. Johansen, D. Milstead, ATL-PHYS-PUB-2006-015
- [22] G. Polesello, A. Rimoldi, ATL-MUON-99-006
- [23] A.Rizzi, CMS-CR-2007/021
- [24] L. Vacavant and I. Hinchliffe, *J. Phys. G: Nucl. Part. Phys.* 27 (2001) 1839-1850
- [25] M. Cvetič and S. Godfrey, "Discovery and Identification of Extra Gauge Bosons", in *Electroweak Symmetry Breaking and Physics Beyond the Standard Model*, eds. T. Barklow, S. Dawson, H. Haber, and J. Seigrist (World Scientific, 1995) p. 383, [hep-ph/9504216].